CHAPTER TWO

REVIEW OF THE CHF PREDICTIONS FOR THE SUBCOOLED FLOW BOILING

In general, there are three kinds of approaches to predict the subcooled flow boiling CHF:

(1) Tabular methods

(2) Empirical correlations,

(3) Mechanistic models

2.1 Tabular Methods

The tabular methods are developed for easy use in the prediction of the CHF. Standard tables of the CHF for pressure, mass flux and subcooling were developed by the USSR Academy of Science (1977), Chalk River Nuclear Laboratories (Groeneveld & Snoek (1984), (1996)). The tables present CHF values at discrete ranges of pressure, mass flux and quality for 8 mm tubes. A correlation is used to account for the diameter effect and to extend the applications to other values of tube diameter. At conditions where the data are scarce or unavailable, CHF values are obtained by extrapolation using the empirical correlations of available data. For the CHF in the tubes other than 8 mm, the CHF is correlated by Doroshchuk et al (1975) as:

$$\frac{CHF_D}{CHF_{D=8mm}} = \left(\frac{D}{8}\right)^n \qquad (2\text{-}1)$$

where CHF_D is the CHF for a diameter of interest, $CHF_{D=8mm}$ is the CHF for a 8mm tube. A value of -0.3 for exponent n is recommended by Celata (1998) and Groeneveld & Snoek (1986).

2.2 Empirical Correlations

The empirical correlations are popular for predicting CHF in the design and the safety analysis for nuclear power plants. The CHF empirical correlations are usually divided into two types: (1) local condition type CHF correlations which are functions of local pressure, mass velocity, subcooling or steam quality, and tube diameter or equivalent hydraulic diameter of the geometric cross section; (2) non-local condition type CHF correlations which are functions of pressure, mass velocity, inlet enthalpy of coolant, heated length and tube diameter or equivalent diameter. Bergles (1963) and Tolubinskiy & Matorin (1973) reported that if the ratio of the tube length effect on the subcooled flow boiling was larger than 20, the tube length effect on the subcooled flow boiling CHF was negligible and the subcooled flow

boiling CHF becomes a local phenomenon. Leung (1980) reported that for a wide range of flow transients, the CHF prediction based on the instantaneous local conditions approach was adequate.

Gunther, Knoebel and Griffel proposed correlations for low and medium pressure condition. The Gunther (1951) correlation is based on the data derived in the tube with 12.7 mm inner diameter and 76 mm heated length. The mass velocity and pressure are controlled in the range 1.5 ~ 12.2 m/s and 0.1~1.1 MPa respectively.

$$CHF = 7.2\times10^{4} V_{l}^{0.5} \Delta T_{lout} \qquad (2\text{-}2)$$

With the data derived in tubes that inner diameter from 7.8 to 11.2 mm, heated length from 508 to 610 mm with coolant mass velocity 4.2 ~ 14.2 m/s and pressure from 0.2 to 0.7 MPa, Knoebel (1973) raised the following correlation:

$$CHF = 48.5\times10^{4}\left(1+0.17V_{l}\right)\left(1+0.124\Delta T_{lout}\right) \qquad (2\text{-}3)$$

And, Griffel (1965) proposed the CHF correlation from the data derived in the tubes with a diameter 5.6 ~ 37.5 mm, heated length 610 ~ 1972 mm, pressure 0.4 ~ 13.8 MPa under mass flux from 1300 ~ 11400 kg/m^{2}s as:

$$CHF = \left(128.7\times G+1.21\times10^{6}\right)\left(8+1.8\Delta T_{lout}\right)^{1.27} \qquad (2\text{-}4)$$

For high-pressure condition, Tong (1969) correlation is based on the data whose pressure ranged form 7 to 14 MPa and mass velocity from 1400 to 4000 kg/m^{2}s.

$$CHF = C_{Tong}\frac{G^{0.4}\mu_{f}^{0.6}}{D^{0.6}}H_{fg} \qquad (2\text{-}5)$$

where $C_{Tong} = 1.76 - 7.433\chi_{eqout} + 12.222\chi_{eqout}^{2}$ (2-5a)

Tong's correlation may also be presented in the form $Bo = \frac{C_{Tong}}{\mathrm{Re}^{0.6}}$, where Bo and Re are boiling number and Reynolds number respectively. The correlation is recommended in the scope that P ≥ 7 MPa.

Inasaka and Nariai (1987) modified the Tong correlation to adapt it to the atmosphere condition.

$$\frac{C_{Inasaka-Nariai}}{C_{Tong}} = 1 - \frac{52.3+80\chi_{eqout}-50\chi_{eqout}^{2}}{60.5+\left(P\times10^{-5}\right)^{1.4}} \qquad (2\text{-}6)$$

The correlation is recommended in the area with pressure from 0.1 to 5.4 MPa. Further, Celata (1994b) modified the Tong correlation as:

$$Bo = \frac{C_{Celata}}{\mathrm{Re}^{0.5}} \quad \text{with} \quad C_{Celata} = \left(0.216 + 4.74\times10^{-2}P\right)\psi \qquad (2\text{-}6a)$$

$$\text{if } \chi_{eqout} > -0.1,\ \psi = 0.825 + 0.986\chi_{eqout} \qquad (2\text{-}6b)$$

$$\text{if } \chi_{eqout} < -0.1,\ \psi = 1 \qquad (2\text{-}6c)$$

$$\text{if } \chi_{eqout} > 0,\ \psi = 1/\left(2 + 30\chi_{eqout}\right) \qquad (2\text{-}6d)$$

The recommendation region for the Celata correlation is:

$$5 \le D \le 8.0mm,\ 12 \le L/D \le 40,\ 0.1 \le P \le 5.0MPa,\ 2.2 \le G \le 40Mg/m^2s,$$

$$15 < \Delta T_{iout} < 190K,\ 4 \le CHF \le 60.6MW/m^2$$

Other important correlation includes W-2 (Westinghouse, Tong, 1968) and W-3 (Tong, 1972). The W-2 correlation is written as:

$$CHF = (0.23\times10^6 + 0.094G)(3 + 0.01\Delta T_{iout})\times[0.435 + 1.23\exp(-0.0093L/D)]$$
$$\times\left\{1.7 - 1.4\exp\left[-0.532\left(\frac{H_f - H_{lin}}{H_{fg}}\right)^{3/4}\left(\frac{\rho_g}{\rho_f}\right)^{-1/3}\right]\right\} \qquad (2\text{-}7)$$

The recommended ranges are:

$0.3 < G < 11$ Mg/m^{2}s, $5.7 < P < 20.0$ MPa, $21 < L/D < 365$,

$0 < \Delta T_{iout} < 126$ K; $1.25 < CHF < 12.5$ MW/m^2.

The W-3 correlation:

$$CHF = \left[2.002 - 0.0000624\mathrm{P} + (0.1722 - 0.0000143\mathrm{P})\times\exp(18.177 - \chi - 0.000599\mathrm{P}\chi\right]$$
$$\times\left[(0.1484 - 1.596\chi + 0.1729\chi|\chi|)\times 0.00073474\mathrm{G} + 1.037\right]$$
$$\times\left[1.157 - 0.869\chi\right]\times\left[0.2664 + 0.8357\exp(-1.241\mathrm{D})\right]\times\left[0.8258 - 0.000341\times\Delta\mathrm{H}_{lin}\right] \qquad (2\text{-}8)$$

where P is in kPa, ΔH_{lin} is in kJ/kg. The correlation is recommended in the ranges:

$$1356 \le G \le 6780Kg/m^2s,\ 6.9 \le P \le 15.9MPa,\ 5 \le D \le 18mm,\ 0.25 \le L \le 3.66m,$$

$$-0.15 \le \chi_{eqout} \le 0.15.$$

2.3 Mechanistic Models

As we know, mechanistic models have the advantage, with respect to the correlations, of being able to characterize not only the existing and developing database, but also to be used to predict CHF beyond the established database. At the moment, according to the basic mechanism assumed by the relative authors as the main cause of the CHF occurrence, major

theoretical approaches to the CHF can be categorized into six groups.

(1) Liquid layer superheat limit model. The difficulty of the heat transfer through the bubbly layer causes a critical superheat in the liquid layer adjacent to the wall, giving rise to the occurrence of the CHF, Tong et al. (1965).

(2) Boundary layer separation limit model. The model is based on the assumption that an injection of vapor from the heated wall into the liquid stream causes a reduction of the velocity gradient close to the wall. Once the vapor effusion increases beyond a critical value, the consequent flow stagnation is assumed to originate the CHF (Kutateladze & Leontiev (1966), Tong (1969, 1975), Purcupile & Gouse (1972), Hancox & Nicoll (1973) and Thorgerson & Knobel (1974)). The weak physical basis of the model has been demonstrated by the studies reported (Fiori & Bergles (1970), Molen & Galjee (1978), Hino & Ueda (1985), and Mattson et al (1973).

(3) Liquid flow blockage model. It assumes that the CHF occurs when the liquid flow normal to the wall is blocked by the vapor flow. Bergelson (1980) considered a critical velocity raised by the instability of the vapor-liquid interface, while Smogalev (1981) considered the effect of the kinetic energy of vapor flow overcoming that of the counter motion of liquid.

(4) Vapor removal limit and near-wall bubble crowding model. It assumed that the turbulent interchange between the core region and the bubbly layer may be the limiting mechanism leading to the CHF occurrence. Hebel et al (1981), Weisman & Pei (1983), and Weisman and Ying (1983) postulate that CHF occurs when the void fraction in the bubbly layer, calculated under the assumption of homogeneous two-phase flow in the bubbly layer, just exceeds the critical value of 0.82. Weisman & Ileslamlou model (1988) is an improvement of Weisman & Pei model for subcooled exit conditions. Recently, Kinoshita (1998) and Kwon (1999) improved the model with introducing new empirical correlations for the calculation of the critical void fraction. The models are unavoidable be of quite empirical due to the determination of the turbulent exchange in the bubbly layer and the core region.

(5) Liquid sublayer dryout model. The model is based on the dryout of a thin liquid sublayer underneath an intermittent vapor blanket, due to coalescent bubbles, flowing over the wall (Lee & Mudarwar (1988), Katto (1990a, 1990b, 1992) and Celata et al (1994a)).

(6) Super heated layer vapor replenishment model. The CHF is postulated to occur when the vapor blanket replenishes the superheated layer, coming into contact with the heated wall, Celata et al (1999).

Currently, only the near wall bubble crowding and the liquid sublayer dryout mechanism are receiving significant attention for the prediction of the CHF.

2.3.1 Bubble-Crowding Model

Fig.2-1 shows the conceptual view of the Weisman-Pei bubble-crowding model. The

model assumes that: A bubbly layer with thickness is adjacent to the tube wall. Bubbles come in from upstream and leave to downstream. Besides, bubbles move radially with enthalpy exchange due to the turbulent radial velocity fluctuation. The CHF occurs when bubble crowding near the heated wall prevents the bulk cold liquid from reaching the wall. The void fraction in the bubbly layer is determined through the balance between the outward flow of vapor bubbles and the inward liquid flow at the bubbly layer-bulk liquid flow interface. In the Weisman-Pei model, the critical condition is that the void fraction in the bubbly layer reaches 0.82, which corresponds to the oval bubbles with long to short radius ratio of 3 to 1 are packed in the bubbly layer. The bubbles are assumed to generate with the bubble detachment diameter by levy model (1967). The thickness of bubbly layer is assumed to be 5.5 times of the bubble detachment diameter, which is determined to fit the CHF experimental data. On the basis of total mass balance and liquid mass balance in the bubbly layer, heat flux q is described as

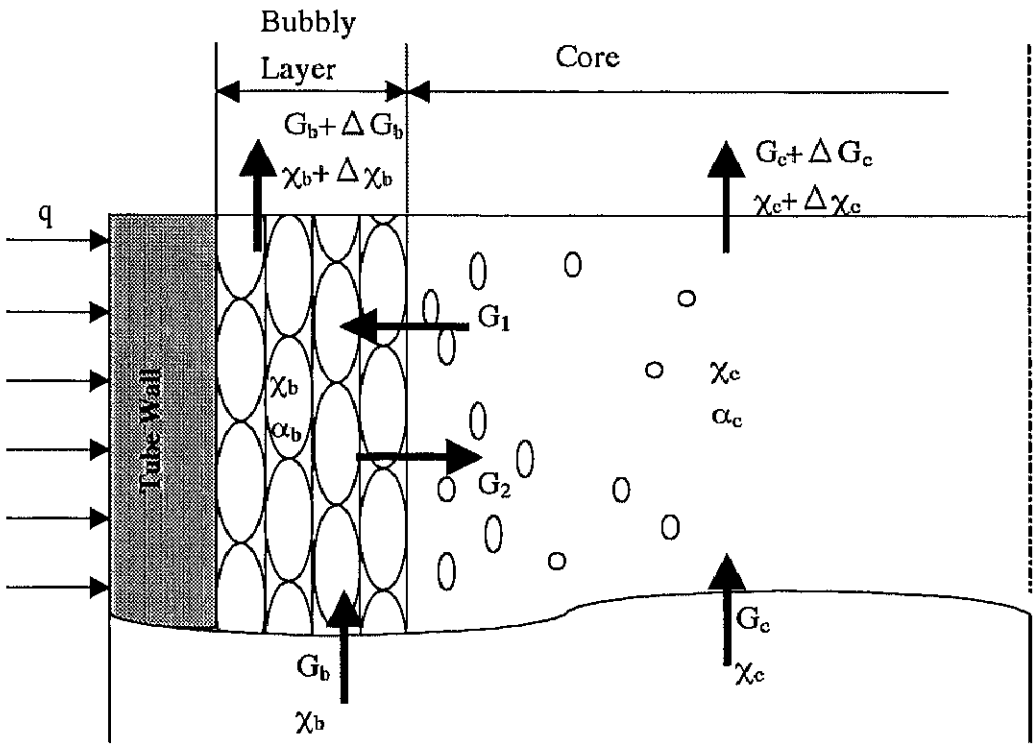

Fig.2-1 Conceptual View of the Bubble Crowding Mechanism in the Weisman-Pei Model

$$\frac{q}{h_{fg}G''}\frac{h_l - h_{ld}}{h_f - h_{ld}} = x_b - x_c \qquad (2\text{-}9)$$

where G'' represents the mass flow rate into the bubbly layer and is determined by the

turbulent velocity fluctuations at the bubbly layer edge, h_l, h_f and h_{ld} are liquid enthalpy, saturated liquid enthalpy and enthalpy at the NVG point respectively. q becomes critical heat flux CHF when χ_b corresponds to critical void fraction, that is, as mentioned above, 0.82.

However, Styikovich et al's measurements (1970) of bubbly layer void fractions at CHF, which shows the void fraction varies from 0.3 ~ 0.95, makes the Weisman-Pei assumption that the critical void fraction is 0.82 quite questionable. It's claimed by Weisman-Pei that the void fraction at CHF maintains quite constant in the range of 0.8 to 0.92 for the heat flux lower than 3.8 MW/m^2 (Water at 3.0 MPa). To overcome the problems, Weisman and Ileslamlou (1988) extended the Weisman-Pei model to high subcooling region using basic energy balance for the bubbly layer to compute the CHF. The applicability of the proposed approach to high-pressure water data (Thompson & Macbeth, 1964), liquid nitrogen data (Papell et al., 1966) and Feron 113 data (Coffield et al., 1969, and Fukayama &Hirata, 1982) are quite good. Currently, the approach of Weisman and coworkers is the only theoretically based CHF prediction procedure that has been shown to give good accuracy with fluids other than water, especially with refrigerants. Prediction of water data at high liquid velocity and subcooling, given in Celata et al. (1994b), shows that, although many data points are predicted within $\pm 30\%$, a clear systematic error is presented. The model tends to over predict the CHF at relatively low heat flux (<20 MW/m^2), while under-predicts CHF at high heat flux (>40 MW/m^2) (Celata et al, 1998).

To adapt the bubble-crowding model better to low L/D condition, Kinoshita et al (1998) modified the Weisman-Pei model by revising the critical void fraction in the bubbly layer α_2 to $\pi/12$. The research reported a good CHF prediction for low-pressure condition.

Recently, Kwon et al (1999) introduced an empirical correlation for the calculation of the critical void fraction in the bubbly layer (eq.2-10). The bubbly layer is assumed as thick as a detached bubble diameter. The model shows a good ability in predicting the CHF in both the subcooled and saturated flow boiling. However, the model calculates the core region two-phase flow average density as equation that is only valid under the homogeneous assumption (eq.2-11). With the equation, obvious abnormal water two phase flow density that may be as high as 4000 is employed in the CHF prediction procedure. The model therefore is considered to be too empirical and in some way not clear enough in physics mechanism.

$$\alpha_b = 0.83 - 0.29\exp(-4.71\chi_{eqout} - 1.89) \qquad (2\text{-}10)$$

$$\rho_{avg} = \frac{\alpha_{avg}\rho_g}{\chi_{avg}} \qquad (2\text{-}11)$$

$$\rho_{avg} = (1-\alpha)\rho_l + \alpha\rho_g \qquad (2\text{-}12)$$

2.3.2 Liquid Sublayer Dryout Mechanism

2.3.2.1 Experimental Base for the Liquid Sublayer Dryout Mechanism

In the case of nucleate boiling at high heat flux, Kusada & Nishigawa (1967), Mesler (1976), Molen & Galgee (1978), Bhat, Prakash & Saini (1983) and Hino & Ueda (1985) experimentally observed that a very thin liquid micro layer was trapped between a vapor blanket formed by the coalescence of several bubbles and the heated wall. The shape of the vapor blanket depended on the geometry of the heater.

Fiori & Bergels (1970), Molen & Galjee (1978) and Hino & Ueda (1985) presented experimental observations of subcooled flow boiling CHF at low pressure, low mass velocity and low or medium subcooling. Fiori & Bergels observed that just before the CHF the wall temperature increased periodically because of bubbles moving past a nucleation site, leading to inadequate cooling of the wall. The CHF occured when the wall temperature increased to exceed the Leidenfrost temperature and prevented further rewetting. They proposed that the thickness of the wall liquid layer was quite large and the water mass entering the liquid layer was greater than the mass evaporating from the wall. The CHF was caused by a hot spot formation in the liquid film during the passage of a slug along the channel.

Molen & Galgee (1978), however, emphasized the role of micro layer evaporation on the CHF. They stated that a very thin liquid layer trapped underneath a coalescent bubble or a vapor slug could be evaporated in a few milliseconds at the CHF. The passage time of a vapor slug of 0.1 second or the residence time of 0.1 second of a bubble layer gave rise to dry areas and the wall temperature increased to exceed the Leidenfrost temperature. This liquid film dryout process prevented rewetting and triggers the CHF.

Hino & Ueno (1985) observed that remarkable large bubbles appear periodically near CHF conditions and that CHF occurs because of micro layer dryout underneath coalescent bubbles. Thus, the large wall temperature rose associated with the CHF results from periodic overheating of the wall to the Leidenfrost temperature.

As a general, the observations can be briefly summarized as:

(1) Large bubbles or vapor slugs are generated by the coalescence of smaller bubbles within two-phase boundary layer in wall region.

(2) Thin liquid micro layer is trapped between the vapor slug and the heated wall.

Based on the above experimental observation, we propose a mechanism sequence of the boiling crisis phenomenon:

(1) Vapor blanket is formed as a consequence of coalescence of small bubbles rising along the near wall region. The vapor blanket moves at a certain speed.

(2) Between the vapor blanket and the tube wall, a very thin liquid sublayer exists.

(3) The liquid sublayer is extinguished during the passage time of vapor blanket.

(4) On the surface covered with a vapor blanket, the heat flux is reduced due to thermal

insulation and the wall temperature rises up to its melting point, resulting the burnout.

Therefore, for the CHF triggering mechanism of the subcooled flow boiling, liquid sublayer dryout mechanism is first raised out by Lee-Mudarwar in 1988.

2.3.2.2 Assumptions of the Liquid Sublayer Dryout Mechanism

Liquid sublayer dryout mechanism for the subcooled flow boiling is principally an extension of Haramura-Katto model (1983) developed for pool and saturated flow boiling. The model assumes that, a vapor blanket, which is formed as a consequence of coalescence of small bubbles rising along the near wall region, is overlying a very thin liquid sublayer adjacent to the wall. The CHF is assumed to happen at the complete dryout of liquid sublayer (fig.2-3). As the result, the CHF can be described as:

$$CHF = \frac{\rho_f \delta H_{fg}}{L_B} U_B \qquad (2\text{-}13)$$

where U_B, L_B, and δ are the vapor blanket velocity, vapor blanket length and thickness of liquid sublayer, respectively. With considering instability wave at the interface I, which is the interface of the liquid sublayer and the vapor blanket (fig.2-3), the length of the vapor blanket is assumed to be equal to the critical Helmholtz instability wavelength, which is inversely proportional to U_B^2 as:

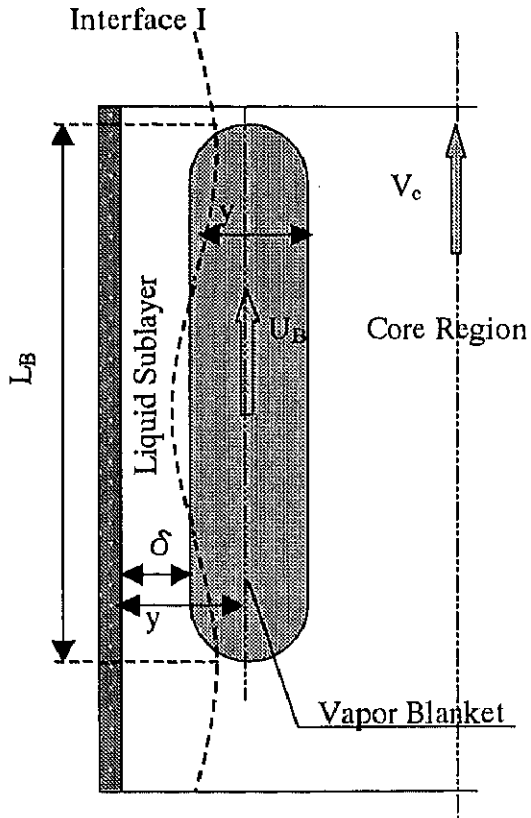

Fig.2-3 Conceptual View of the Liquid Sublayer Dryout Mechanism

$$L_B \propto \frac{1}{U_B^2} \qquad (2\text{-}14)$$

Then the CHF is written in:

$$CHF = KU_B^3\delta \qquad (2\text{-}15)$$

where K is a proportional constant and diverses in different model. From the eq.2-15, we find that the key for the liquid sublayer dryout mechanism turns to be the calculation of the U_B and the calculation of the δ. Different models employed different ways.

2.3.2.3 Main Previous Work for the Liquid Sublayer Dryout Mechanism

2.3.2.3.1 Lee-Mudarwar Model (1988)

In the Lee-Mudarwar model, the liquid sublayer thickness δ is calculated from a force balance on the vapor blanket in the radial direction. The rate of momentum produced by sublayer evaporation into the vapor blanket, which pushes the vapor blanket away from the wall, is balanced by a lateral force caused by the rotation of the blanket due to the relative velocity between the two phases and the velocity gradient associated with the liquid boundary layer. On the base of the sublayer thickness, the liquid velocity at the centerline of the vapor blanket, U_{BL}, is obtained from Kaman velocity distribution equations. U_B is then calculated as the sum of the liquid velocity at the centerline of the vapor blanket, U_{BL}, and the relative vapor blanket velocity determined by the balance between buoyancy and drag forces exerted on the vapor blanket. Three empirical constants are employed in the model. The first is used in the analysis for evaluating the temperature of the liquid entering the sublayer. The other two are used in the analysis for evaluating the lateral force on the vapor blanket necessary to calculate the sublayer thickness. The three empirical constants are evaluated through the comparison with the experimental data. Although it can closely predict several well-known databases which are characterized by high pressure and low mass velocity ($4.9 < P < 17.6MPa$, $4 < D < 16mm$, $1000 < G < 5000kg/m^2s$, $\Delta T_{in} < 50K$, $\alpha < 0.7$), the model was found to be unable to give accurate CHF predictions at low pressure (Celata, 1994b).

2.3.2.3.2 Katto Model (1990a, 1990b, 1992)

Katto evaluated δ using a correlation for pool boiling (Haramura & Katto, 1983, eq.2-16) and calculated U_B by using empirical based relation (as a function of liquid & vapor densities and void fraction as eqs.2-17 and 2-18). The Katto model, although yielding acceptable predictions of very high CHF data points in a wide range of pressure, and having the capability to apply to not only water but also various non-aqueous fluids (such as R-11, R-12, R-113, Nitrogen and Helium), is not able to calculate the CHF in those cases where the local void fraction in the near-wall bubbly layer is higher than 70%. This is the limit for the

validity of the assumption of homogeneous flow in the bubbly layer. It happens in all cases where inlet thermal hydraulic conditions are such that the bulk liquid at the exit is slightly subcooled (Celata, 1994b).

$$\delta = \frac{\pi(0.0584)^2}{2}\left(\frac{\rho_g}{\rho_f}\right)^{0.4}\left(1+\frac{\rho_g}{\rho_f}\right)\frac{\sigma}{\rho_g}\left(\frac{\rho_g H_{fg}}{q_b}\right)^2 \qquad (2\text{-}16)$$

where q_b is boiling heat flux

$$U_B = kU_\delta \qquad (2\text{-}17)$$

where U_δ is local velocity of homogeneous two-phase flow at distance δ from the wall. k is an empirical velocity coefficient and is written as:

$$k = \frac{242[1+K_1(0.355-\alpha)]}{\left[0.0197+\left(\frac{\rho_g}{\rho_f}\right)^{0.733}\right]\left[1+90.3\left(\frac{\rho_g}{\rho_f}\right)^{3.68}\right]}R_e^{-0.8} \qquad (2\text{-}18)$$

where $K_1 = 0$ for $\alpha > 0.355$; $K_1 = 3.76$ for $\alpha < 0.355$.

2.3.2.3.3 Celata Model (1994a)

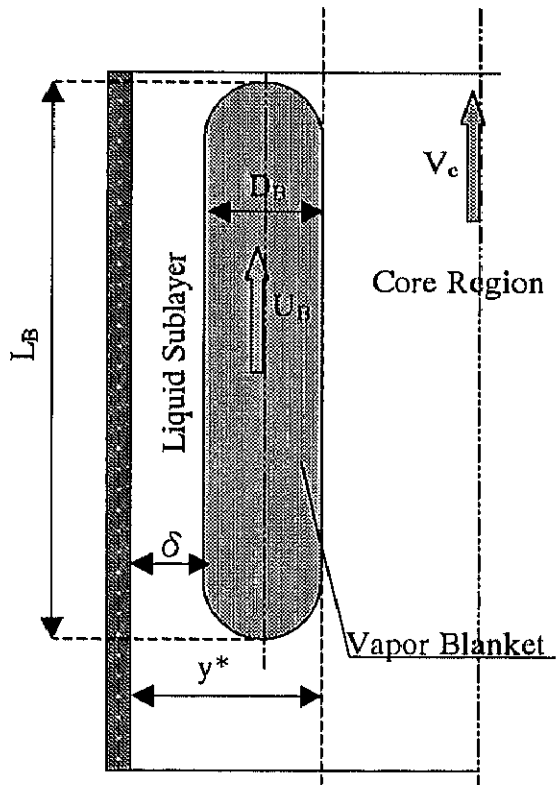

Fig.2-4 Conceptual View of the Liquid Sublayer Dryout Mechanism in Celata Model (1994)

Celata et al (1994a, fig.2-4) assumed that the vapor blanket developed and existed only

in the near-wall region where the local liquid temperature was higher than saturation temperature. δ is calculated by subtracting the vapor blanket diameter D_B from superheated liquid thickness y*. With δ calculated, the U_B is computed as what in the Lee-Mudarwar model. The model is successful in predicting the CHF at low-medium pressure and for the fist time, no empirical constant is employed in the calculation process. However, the model shows deficiency in the CHF prediction at low L/D condition (Kinoshita et al. 1998) or at high-pressure condition.

Recently, Celata (1999) raised a superheated layer vapor replenishment model. The new model approaches CHF almost the same procedure and therefore results in almost same CHF prediction as the old one. It still cannot overcome the defect mentioned above.

As mentioned in the chapter 2.3.2.1, for the most often encountered flow pattern near the CHF, based on the experimental observations reported in the previous works, the liquid sublayer dryout mechanism is adopted as the CHF triggering mechanism by the present author. And in view of the above-described limitations of the Lee-Mudarwar, Katto and Celata models, a new mechanistic model is developed for the CHF prediction with the aim of accuracy, simplicity and clear physics meaning.